scientific reports

Check for updates

OPEN

A non-metallic PEEK topology optimization reconstruction implant for large mandibular continuity defects, validated using the MANDYBILATOR apparatus

Bram B. J. Merema✉, Frederik K. L. Spijkervet, Joep Kraeima & Max J. H. Witjes

In cases of large mandibular continuity defects resulting from malignancy resection, the current standard of care involves using patient-specific/custom titanium reconstruction plates along with autogenous grafts (fibula, scapula, or iliac crest segments). However, when grafts are not feasible or desired, only the reconstruction plate is used to bridge the gap. Unfortunately, metal osteosynthesis and reconstruction plates, including titanium, exhibit adverse effects such as stress-shielding and limitations in accurate postoperative irradiation (especially with proton-beam therapy). To address these issues, in this study we explore, develop and validate a non-metallic solution: a topology-optimized polyetheretherketone (PEEK) load-bearing implant for large non-grafted mandibular continuity defects. In order to thoroughly validate the developed PEEK reconstruction, a dedicated MANDYBILATOR testing apparatus was developed. Using the MANDYBILATOR finite element analysis results of the implant were confirmed and the PEEK implant was mechanically validated for both static and dynamic loading. Results show that the PEEK reconstructed mandible is comparably strong as the unreconstructed mandible and is unlikely to fail due to fatigue. Our PEEK implant design has the mechanical potential to act as a substitute for the current titanium plates used in the reconstruction of continuity defects of the mandible. This may potentially lead to optimised patient-specific reconstructions, with the implants matching the bone's stiffness and possessing radiolucent properties which are useful for radiographic follow-ups and radiotherapy. Furthermore, the addition of the dynamic/cyclic MANDYBILATOR apparatus allows for more realistic application of the in-vivo loading of the mandible and can provide added insights in biomechanical behaviour of the mandible.

The preferred approach when reconstructing continuity defects of the mandible following tumour resection is generally to bridge the defect using an autogenous free vascularised bone flap, such as a fibula or scapula graft, which is fixated to the mandibular segments using osteosynthesis materials (OSM) in the form of rigid titanium reconstruction plates (RP) or mini plates. When patients are unfit to undergo a free vascularised bone flap reconstruction due to the poor quality of the donor site's vascularisation, an impaired medical condition or refusal to undergo major free vascularised bone flap surgery, the continuity defects are generally reconstructed with merely a RP. These can either be manually contoured conventional plates or patient-specific implants (PSI). Reported complications in the reconstruction of continuity defects of the mandible using RPs are plate fracture, screw loosening, intra- and/or extra-oral plate exposure and stress-shielding[1–5].

As the human mandible is a complex and relatively heavily loaded anatomical structure, such reconstruction plates are made from high performing metals. The most used materials nowadays are commercially pure titanium and titanium alloys, as they are strong, lightweight, biocompatible and have a good resistance to fatigue. However, the titanium alloys used for mandibular reconstructions are also rather stiff when compared to the human cortical bone. These alloys have a Young's elastic modulus of approximately 110 GPa, whereas mandibular cortical bone remains around 4–20 GPa[6,7]. As a result of this mismatch in material stiffness, the mandible can locally be subjected to under-straining upon postoperative loading of the reconstructed mandible as the neighbouring titanium is stiffer. This effect is called stress-shielding and, according to Frost's 'Mechanostat' principle, it can

Department of Oral and Maxillofacial Surgery, University Medical Center Groningen, University of Groningen, Hanzeplein 1, P.O. Box 30.001, 9700 RB Groningen, The Netherlands. ✉email: b.j.merema@umcg.nl

disturb the natural equilibrium of the local bone's strain values, and bone formation or resorption[8,9]. As a result of stress-shielding, bone resorption can occur at or close to the bone-implant interface, ultimately leading to potential screw loosening and failure of the reconstruction[10].

Apart from the mismatch in elastic modulus between bone and the commonly applied titanium alloys, a limitation of titanium and other metallic plates is their interference with radiological imaging. Due to backscattering and metal streak artefacts, both postoperative radiological imaging and radiotherapy become suboptimal and less accurate since the signal gets absorbed or distorted due to the dense metallic material[11]. Moreover, most patients whose continuity defect has been reconstructed after the removal of a malignity, subsequently undergo radiotherapy but the metallic reconstruction interferes with the delivery of photons or protons to the target tissues and inadvertently can increase the dose in the neighbouring areas. This complicates postoperative radiotherapy and the VSP of potential secondary reconstructions.

A solution for aforementioned limitations could be to develop a reconstruction made from a radiolucent material which is comparable in stiffness as the bone[11]. Such properties can be found in high performing polymers. Hence, polymeric implants have been discussed in the literature as potential substitutes for metallic OSM but, due to their limited strength compared to the common implant metallic materials, they are generally found unfit for the reconstruction of rather large and heavily loaded defects, such as a continuity defect of the mandible.

Typical examples of high performing biocompatible polymers are polyetheretherketone (PEEK) and polyetherketoneketone (PEKK), both found within the polyaryletherketone (PAEK) family. PEEK has been used as a material for non-load-bearing applications e.g., augmentations and cranioplasties, for several decades already and have shown excellent biocompatibility. However, due to their mechanically inferior material properties, PEEK and PEKK are generally deemed unfit for heavily loaded implant constructs[12]. Recently, an attempt has been made to manufacture a load bearing construct for the reconstruction of mandibular continuity defects, however, unsuccessful in terms of being able to withstand the physiological loading of the mandible[13]. In that study, a conventional strip-like plate was manufactured that was similar in shape to titanium reconstruction plates, which possibly may not have been the optimal design for a PEEK reconstruction. Alternatively, a geometrically optimal structure, designed to be manufactured from a high performing polymer, could provide a sufficiently strong load bearing construct. A method that can be used to obtain such a geometrically optimal structure is topology optimisation[14–16]. Using finite element analysis (FEA) combined with topology optimisation, a load driven design can be realised by means of a solid design space or volume from which material is removed from the lower stressed areas. This way, a design dedicated to the analysed material can be realised.

In order to thoroughly validate such a novel PEEK reconstructive PSI, we develop two apparatus, one for static experiments and one for dynamic cyclic loading. Using these, we obtain insights in both the ultimate strength and the fatigue behaviour of the PEEK reconstruction. We hypothesise that a full PEEK PSI, obtained through thorough finite element analysis and subsequent topology optimisation, can withstand the in-vivo loading of the mandible and act as a substitute for current titanium plates in the reconstruction of continuity defects of the mandible.

Materials and methods

A representative deceased head and neck oncological subject with a class II Brown's[17] or Jewer L-type[18] mandibular defect was selected as an exemplar case. This 70-year-old male subject was edentulous and his mandibular body had already decreased slightly to a height of 22 mm. The defect size was selected as it is most prone to failure, according to the Shibahara et al. study[5]. Based on experience of the team, the design space, the boundary volume for the topology optimisation process to remove volume from, was designed at 2.5 mm and 8.5 mm lower than the resected segment at the posterior and anterior osteotomy sites, respectively to allow for space for proper soft tissue closure. A number of potential screw positions was chosen manually, in agreement with an experienced head and neck oncology oral and maxillofacial surgeon (MJHW). Based on the findings in our prior work[19], where adding screws in the osteotomy sites had a positive effect on the internal stresses in the implant, a stress-reducing screw was incorporated into both of our subject's mandibular. Two strategically chosen screws need mentioning; the bookshelf screw[19] and a newly defined dual locking sandwich-screw, which was designed to allow for a bi-cortical locking screw to be supported and locked on both the buccal and lingual side of the mandible. Due to this dual locking principle, the implant is supported on both sides of the mandible without applying resorption-inducing pressure to the sandwiched bone[20,21]. This dual locking sandwich-screw can be inserted laterally after the guided pre-drilling of the screw pilot holes. (Fig. 2). Initially, many screws, namely 23, were put in the FEA model so that any screw that proved unnecessary through topology optimisation could be removed at a later stage.

In order to approach the dynamic loading statically at various angles of the mouth opening, a number of scenarios was constructed. Four different mandibular orientations were chosen, i.e., maximum occlusion and 5- 10- and 15 degrees of mouth opening. Three bite positions were considered for each mandibular orientation, the incisal and left and right premolar regions. This resulted in a total of 12 different loading scenarios.

Recently, we published a protocol for the 3D determination of PS muscle models of the jaw elevators[22]. This protocol combines MRI muscle delineation, bite force measurements and FEA in order to extract each specific PS muscle force. As we could not perform bite force measurements on the selected deceased subject, it was chosen to create a hybrid muscle model based on that protocol. This hybrid muscle model was obtained by combining the PS muscle orientations and directions together with the literature based maximum muscle forces[23]. Using the available MRI, the elevator muscles were delineated in the Brainlab 2020 software (Brainlab, München, Germany) using the SmartBrush tool (version 3.0) and the origin and insertion sites were determined to find each muscle's acting direction in the form of a vector. These vectors were then scaled to match the muscle forces reported by Langenbach and Hannam[23], which were based on the work by Weijs and Hillen[24]. These

Literature based muscle model used in FEA models		MS		MP		PM		TA		TM		TP	
		R	L	R	L	R	L	R	L	R	L	R	L
Occlusion	x	-84.3	71.2	-20.5	18.2	53.7	-52.0	-36.0	32.6	-35.5	38.3	-55.2	56.8
	y	166.6	174.3	72.4	75.1	149.8	138.5	153.8	154.4	86.7	85.2	48.0	45.8
	z	37.7	28.9	31.9	26.3	72.5	93.3	5.6	8.6	-19.7	-20.6	-19.6	-20.1
	F.res	190.5	190.5	81.7	81.7	174.9	174.9	158.0	158.0	95.7	95.7	75.7	75.7
5 Degrees opening	x	-90.6	78.0	-21.8	19.5	64.4	-62.1	-31.8	28.1	-34.9	37.8	-54.0	55.7
	y	163.7	171.7	72.7	75.4	147.4	137.1	154.7	155.3	87.1	85.8	49.6	47.4
	z	35.6	27.1	30.1	24.8	68.7	89.0	5.4	8.1	-18.6	-19.3	-18.9	-19.4
	F.res	190.5	190.5	81.7	81.7	174.9	174.9	158.0	158.0	95.7	95.7	75.7	75.7
10 Degrees opening	x	-96.8	84.7	-23.3	20.9	74.5	-71.7	-28.9	24.8	-33.9	36.8	-52.7	54.5
	y	160.5	168.7	72.9	75.4	144.1	134.9	155.3	155.9	87.7	86.4	51.2	49.1
	z	33.9	25.5	28.6	23.4	65.3	85.2	5.1	7.5	-17.7	-18.2	-18.3	-18.7
	F.res	190.5	190.5	81.7	81.7	174.9	174.9	158.0	158.0	95.7	95.7	75.7	75.7
15 Degrees opening	x	-103.0	91.4	-25.1	22.6	84.0	-80.7	-27.0	22.7	-32.7	35.6	-51.3	53.2
	y	156.9	165.4	72.8	75.3	140.2	131.9	155.6	156.2	88.3	87.1	52.8	50.8
	z	32.4	24.1	27.2	22.1	62.3	81.8	4.9	7.1	-16.9	-17.3	-17.7	-18.1
	F.res	190.5	190.5	81.7	81.7	174.9	174.9	158.0	158.0	95.7	95.7	75.7	75.7

Table 1. Muscle orientations and directions derived by means of delineation of the patient's MRI. The muscle forces were taken from the literature[23]. The three-dimensional force vectors were broken down into x, y and z components for both lateralities of the masseter superficialis (MS) and masseter profunda (MP), pterygoideus medialis (PM) and temporalis- anterior (TA), middle (TM) and posterior (TP) muscles. The Frankfurt horizontal plane (FHP) functioned as the x–z plane with its positive x-axis pointing towards the left condyle, the positive y-axis pointing cranially and the positive z-axis pointing ventrally. The origin of the coordinate system was set where the mid-sagittal plane coincided with the FHP.

	CSA (cm^2)		Muscle force (N) F = 37 * CSA	
Muscle	R	L	R	L
Masseter superficialis	4.1	3.6	152.4	134.3
Masseter profunda	2.1	2.3	78.4	86.2
Pterygoideus medialis	3.2	3.0	118.8	111.0
Temporalis	5.8	5.4	214.6	198.3

Table 2. The cross-sectional areas (CSAs) that were determined from the MRI together with the specific muscle forces that were calculated using the intrinsic strength value (37 N/cm^2) taken from the literature[24].

muscle vectors were then recalculated for the 5-, 10- and 15 degrees mouth opening scenarios, by connecting the original muscles' origins on the skull to the insertion sites on the opened mandibles, resulting in a total of 48 unique muscle vectors. Table 1 shows the muscle vectors of this hybrid model for these scenarios at four different mandible orientations. It should be emphasised that our hybrid method uses literature based muscle forces for dentate patients and so are probably higher than this specific patient's were[22]. The Frankfurt horizontal plane (FHP) functioned as the x–z plane with its positive x-axis pointing posteriorly, the positive z-axis pointing towards the right side of the mandible, and the y-axis pointing cranially. The origin of the coordinate system was set where the mid-sagittal plane coincided with the FHP.

Following the prior PS muscle model determination protocol presented by Merema et al.[22], the muscle directions and forces were determined in a PS manner for comparison purposes. An intrinsic strength value of 37 N/cm^2 was used to convert the muscle cross-sectional area (CSA) from the MRI to muscle force[24]. Tables 2 and 3 describe this PS muscle model.

FEA was performed in Solidworks 2020 Premium version SP5.0 (Dassault Systèmes SolidWorks Corporation, Waltham, MA, USA). On each condyle, a single node was fixed in space (x, y & z) while, depending on the specific scenario, the bite region (circular area of 7 mm^2) was fixed in only the z-direction, the caudal-cranial axis. Bonded intercomponent connections were chosen between all the touching components i.e., mandibular cortical and cancellous components, screw cylinders and the implant itself. The implant design space was designed to be offset at 0.1 mm to the bone and was connected to the mandibular segments by means of two-sectioned concentric cylinders to allow for a pin-joint semi-contact to improve the optimisation quality after topology optimisation. The mandibular model was obtained through segmentation of the subject's CT-scan. The cortical portion was segmented in the Mimics 22.0 software (Materialise, Leuven, Belgium) and the inner

Patient specific Cyclic test 15 degrees molar	MS		MP		PM		TM	
	R	L	R	L	R	L	R	L
x	-82.4	64.5	-24.1	23.9	57.1	-51.3	-73.3	73.8
y	125.5	116.6	69.9	79.5	95.2	83.7	198.1	180.6
z	25.9	17.0	26.1	23.4	42.3	51.9	-37.9	-35.8
F.res	152.4	134.3	78.4	86.2	118.8	111.0	214.6	198.3

Table 3. The three-dimensional force vectors that were used for the cyclic test were translated from the PS MRI measurements (Table 2).
The muscle forces were broken down into x, y and z components for both lateralities of the masseter superficialis (MS) and masseter profunda (MP), pterygoideus medialis (PM) and middle temporalis (TM) muscles. The Frankfurt horizontal plane (FHP) functioned as the x–z plane with its positive x-axis pointing towards the left condyle, the positive y-axis pointing cranially and the positive z-axis pointing ventrally. The origin of the coordinate system was set where the mid-sagittal plane coincided with the FHP.

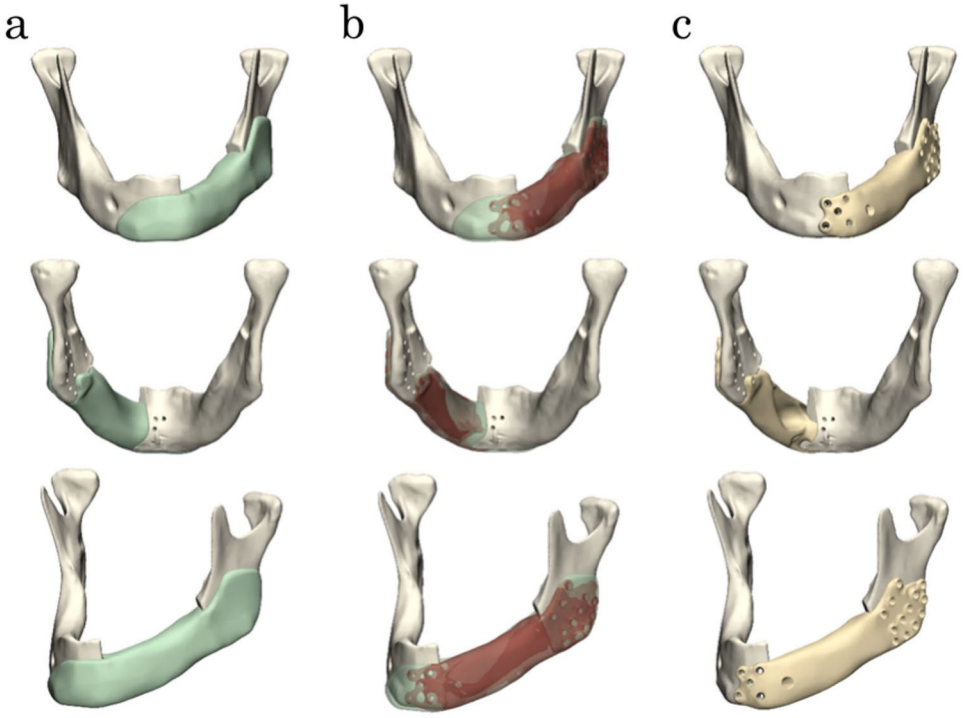

Fig. 1. Visualisation of the topology optimisation process. (**a**) The design domain in green, (**b**) the result of the topology optimisation in red, (**c**) the finalised implant, adapted for manufacturing through milling, in beige.

cavities were assigned as cancellous bone. The homogeneously (isotropic linear elastic) mechanical properties of cortical bone (E = 14.7 GPa, ν = 0.3), cancellous bone (E = 400 MPa, ν = 0.3), Ti-6Al-4 V titanium screws (E = 110 GPa ν = 0.31), PEEK (E = 3.6 GPa, ν = 0.4) were applied to the models, in agreement with the work by Mesnard and Ramos[25–29].

The results of all 12 FEA studies were exported in .INP format and imported into the ProTOp 6.1 software (CAESS, Maribor, Slovenia) for topology optimisation. The optimisation objective was set to minimum strain energy, to exhibit the lowest possible stress values. ProTOp assigns a weighing factor to each input FEA scenario, indicating the most dictating scenario in the optimisation process. In our study, the molar bite scenarios were the most dictating in terms of peak stress values in the implant. The output topology optimised volume, however, was optimised to conform all input bite scenarios. After the topology optimisation was finished, resulting in an optimised implant within the provided design space and sufficient for all 12 loading scenarios, the optimised structure was exported to the 3-Matic version 15.0 software (Materialise, Leuven, Belgium) in STL format. Within 3-Matic, the design was optimised for 4-axis milling and finalised for manufacturing (Fig. 1). Two identical implants were milled by Witec Medical (Stadskanaal, The Netherlands) from ZELLAMID® 1500 X PEEK (Senova, Uttendorf, Austria). The corresponding mandibular segments were manufactured and assembled to the PEEK implant using 2.7 mm ThreadLock locking screws (KLS Martin, Tuttlingen, Germany) before undergoing the static and cyclic mechanical testing (Fig. 2).

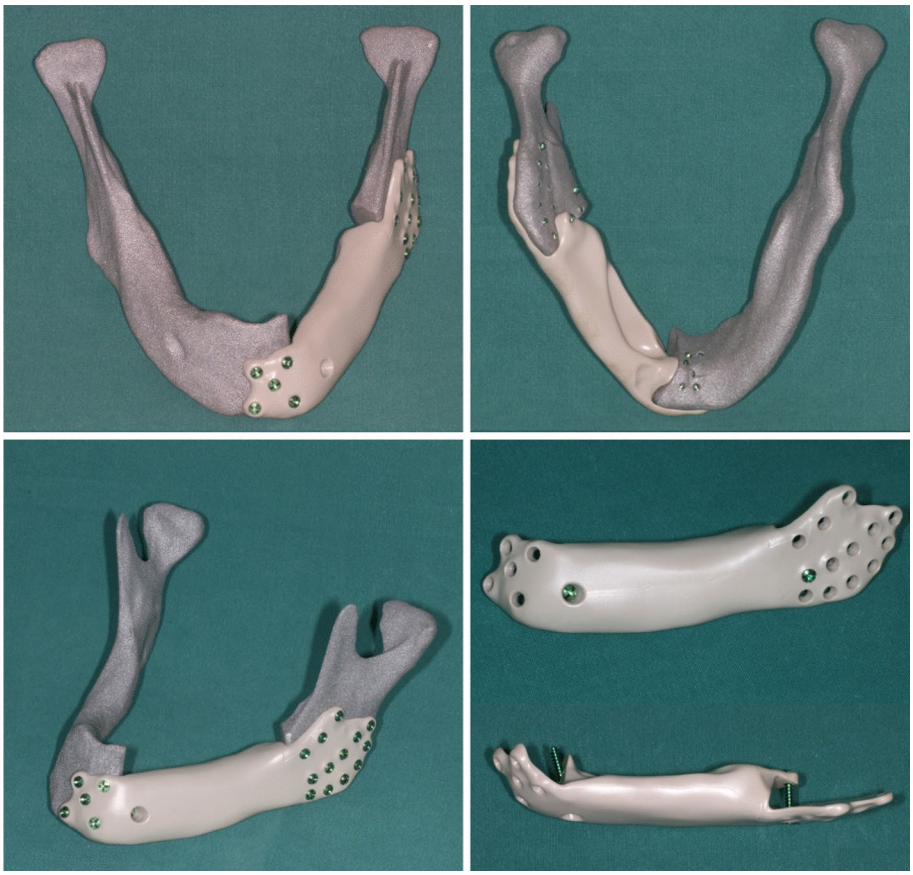

Fig. 2. One of the milled PEEK implants together with the In-VitroBone synthetic mandible. This sample was used for static testing on the MUNACAPP apparatus. The lower right image gives a good view of the two strategically placed screws.

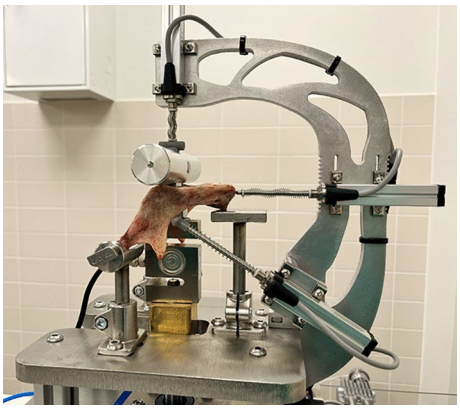

Fig. 3. A picture of the MUNACAPP apparatus ready for static uniaxial compressive testing of a cadaveric mandible.

Mechanical testing apparatus

As commercially available synthetic mandibles were developed for surgical training purposes, their mechanical properties deviate substantially from human bone, by a factor of 10–20[15]. Also, they are not manufactured patient-specifically, therefore, we found them to be unsuitable for our experiments. In order to allow for mechanical testing with PS shaped mandibles, we chose to develop a synthetic bone substitute, In-VitroBone. A mechanical tensile testing apparatus was developed for this purpose, the Mandibular UNiAxial Compression testing APParatus (MUNACAPP) device shown in Fig. 3. The device mimics the mandibular elevator muscle forces in a simplified manner by means of one resulting force, which is applied to both mandibular angles,

and is the most commonly found mandibular testing setup in the literature[15,30–33]. Even though this is an oversimplification of the anatomical situation, it provides easily comparable data due to its minimalistic setup.

In order to carry out more anatomically correct loading experiments of the patient-specific mandible and corresponding muscle model, a MANdibular DYnamic BIte simulator (MANDYBILATOR) apparatus was developed in-house. As the most common type of mandibular mechanical testing setup is oversimplified, as aforementioned, we decided to develop an apparatus that allows for individual mandibular muscle direction, force and activation, thereby accurately mimicking the specific patient or subject's biomechanical situation. Eight elevator muscles were assigned to the current experiment: the masseter superficialis and masseter profunda, and the pterygoideus medialis and temporalis muscles from both lateralities. The pterygoideus lateralis muscles were not included as both condyles were not mobile in this experiment. Each muscle direction and force could be replicated by electro-pneumatically controlled muscles, which consisted of a bellow component (Festo, Esslingen am Neckar, Germany) and a load cell to measure the individual muscle forces. Aramide ropes, connecting the artificial muscles to the muscle insertions, were glued to each muscle insertion area on the mandible, corresponding to the MRI data and FEA model. Both condyles were supported by artificial glenoid fossae, which were 3D printed polyamide cups (PA12, Oceanz, Ede, the Netherlands) with an imprint of the condyle connected to a seesaw construct to reverse the vertical condylar reaction force direction. At the other end of the seesaw constructions, two load cells were applied to measure the resulting condylar forces. The mandible was cranio-caudally constrained in the dental arch by means of a 3D printed (PA12) cup fixed to a sling around the alveolar process. Another load cell was applied to this sling, enabling bite force measurements. The sling could be positioned throughout the dental arch to accommodate for, e.g., incisal, canine, premolar or molar bite positions. The device could be deployed in both a static and a dynamic manner, enabling cyclic or fatigue testing.

A small series of fresh frozen human cadaveric mandibles were harvested, CT-scanned and frozen again. Using the CT images, synthetic, In-VitroBone clone mandibles were created. Tensile experiments were performed on the MUNACAPP apparatus by loading both the cadaveric mandibles and their synthetic In-VitroBone clones in the exact same manner. During the experiments the tensile force and corresponding vertical displacement as well as displacement at the pogonion and external oblique line of each mandible were measured and recorded. We found that the In-VitroBone mandibles failed within 1.5 percent of the ultimate tensile force of their cadaveric mandibles. Due to its lower Young's modulus of elasticity, the In-VitroBone tended to deform more prior to failure, as it was slightly less stiff than the anatomical mandibular construct. This feature we were willing to accept as it introduced a worst-case scenario by loading the implant in a less favourable manner than the cadaveric bone. Figure 4 shows the MANDYBILATOR apparatus with an In-VitroBone test sample mounted.

Validation of the apparatus

Directly after setting up the MANDYBILATOR apparatus with the PEEK implant reconstructed synthetic mandible test sample (see Fig. 5), all the actuating muscle forces together with the resultant forces on both condyles and the bite force were measured to validate the apparatus. This was done in both a static and cyclic setting. A three second ramp load was recorded for static validation of the individual muscle forces and the resulting forces on both condyles and the molar bite position. All the recorded forces were then compared to their targets, i.e., the muscle forces that were inputs for the FEA model of the dynamic test situation (Table 2) and the resulting forces on both condyles and the molar bite position that were the results of this FEA.

Subsequently, a cyclic validation test was performed at a frequency of 1 Hz, the frequency of the dynamic experiment. In this test, the bite force and both condylar forces were measured and compared to the results of the matching predictive FEA. This test was repeated directly after the initial experiment had finished, at 500,000 cycles, the equivalent number of chewing cycles with considerable bite force during approximately two years of in-vivo use[13].

Experiments

Two experiments, one static and one dynamic, were designed to assess the durability of the PEEK implants. The static ultimate performance experiment was performed first on the MUNACAPP apparatus. Three intact mandibles (n = 3) and three exact duplicates with the continuity defect (n = 3) were all manufactured from In-VitroBone. The continuity defects were reconstructed with the topology optimised PEEK implant and 2.7 KLS screws prior to testing in the static setup. The device was adjusted so that the mandibles rested on both condyles

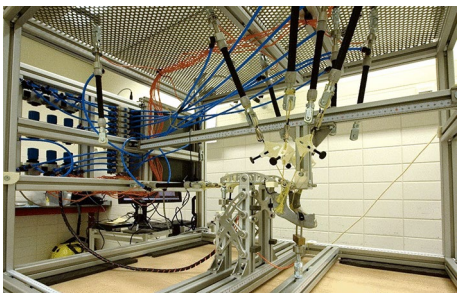

Fig. 4. Overview of the complete MANDYBILATOR apparatus with the mandible situated in the lower middle, the artificial muscles in the top middle and the electro-pneumatic controls on the left side.

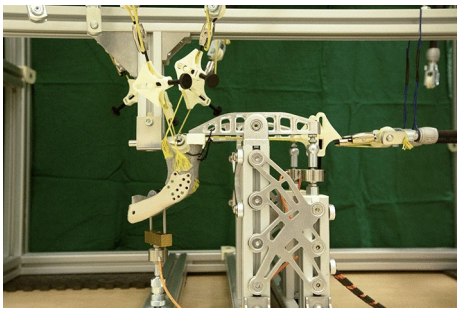

Fig. 5. Close up of the PEEK reconstructed mandible places inside the MANDYBILATOR apparatus, ready for cyclic testing. Note that only four screws are inserted in the left ramus of the mandible throughout mechanical testing of the implant.

and the incisal position on the alveolar process was in an approximately occlusal orientation. A self-balancing round bar (D = 32 mm) was used to apply the vertical resultant muscle force to both mandibular angles equally. A pre-load of approximately 30 N was applied prior to each experiment. The load was gradually increased by approximately 17 N per second until failure occurred. Throughout the experiments, the applied vertical load (N) and displacement (mm) were registered together with linear displacements at the pogonion and mandibular lateral oblique line (mm). The applied force was registered by an S-type load cell while the displacements were measured through linear potentiometers. The ultimate load at failure was used as a measure of the mandible's strength while the ultimate displacements provided an insight into the stiffness of the mandible.

Subsequently, cyclic performance experiments were performed on the MANDYBILATOR apparatus, which had been developed in-house for this specific purpose. Another PEEK reconstructed In-VitroBone mandible was positioned in the occlusal orientation and the muscle vectors were adjusted in conformation with the vectors listed in Table 1 under *Occlusion, MRI CSAs*. The bite position was set to the right molar position at 15 degrees of mouth opening, as, according to the topology optimisation study, this represents the worst-case out of the 12 loading scenarios. The load was set to fluctuate from nearly 0 N to the subject's full bite capacity, as shown in Table 2, which is a semi-PS muscle model based on the subject's MRI CSAs, muscle directions and the intrinsic strength value of 37 N/cm^2[24]. This resulted in the force components presented in Table 3. The load frequency was set to 1 Hz with 800 ms of 'muscle' activation, followed by 200 ms relaxation, for a maximum number of 500,000 cycles, which is in agreement with the experiments performed by Lang et al.[16]. According to Lommen et al., this is equivalent number of chewing cycles with considerable bite force during approximately two years of in-vivo use[13]. All the inserted screws were marked using a marker prior to the dynamic experiment, allowing for the observation of early stage screw loosening. As the PEEK implant covered the insertion site of the master superficialis muscle, this muscle was not attached during the dynamic experiment in the MANDYBILATOR apparatus.

The cycle at which the reconstruction failed mechanically, irrespective of whether the cause was implant failure or screw loosening, was considered the final failure cycle.

Data collection and outcomes

The data was collected by an Arduino Mega microcontroller (Arduino, www.arduino.cc, accessed on 18th of April 2023) and written into a .CSV file in real-time. The program measured at a frequency of 10 Hz. and was programmed to loop 100 measurements followed by 900 skipped measurements, to maintain an acceptable file size.

Results

Validation of the MANDYBILATOR apparatus

The ramp load, applied for static validation of the MANDYBILATOR apparatus, showed that all the set-up muscle forces lay within 1% of their target values, as depicted in Table 2. Figure 6 visualises this static validation.

The cyclic validation, performed both directly prior to and subsequently after the 500,000 cycles dynamic experiment, shows that the resulting forces on the bite position and both condyles, as measured in the MANDYBILATOR apparatus, resemble the FEA predicted values well. Prior to the 500,000 cycles dynamic experiment, the MANDYBILATOR showed forces of 141.5 N, 213.6 N and 476.4 N while the outcomes of the FEA predicted 150.6 N, 217.2 N and 475.2 N for the right condyle, left condyle and molar bite force respectively. This translates to an error of 6%, 2% and 0% respectively, between the FEA predicted values and experimentally measured values. Figure 7 visualises these results.

Directly following the dynamic experiment, the MANDYBILATOR measured forces of 154.1 N, 207.5 N and 450.3 N after 500,000 cycles for the right condyle, left condyle and molar bite force, respectively. This indicates that the consistency of the MANDYBILATOR apparatus over 500,000 cycles lies within 10%.

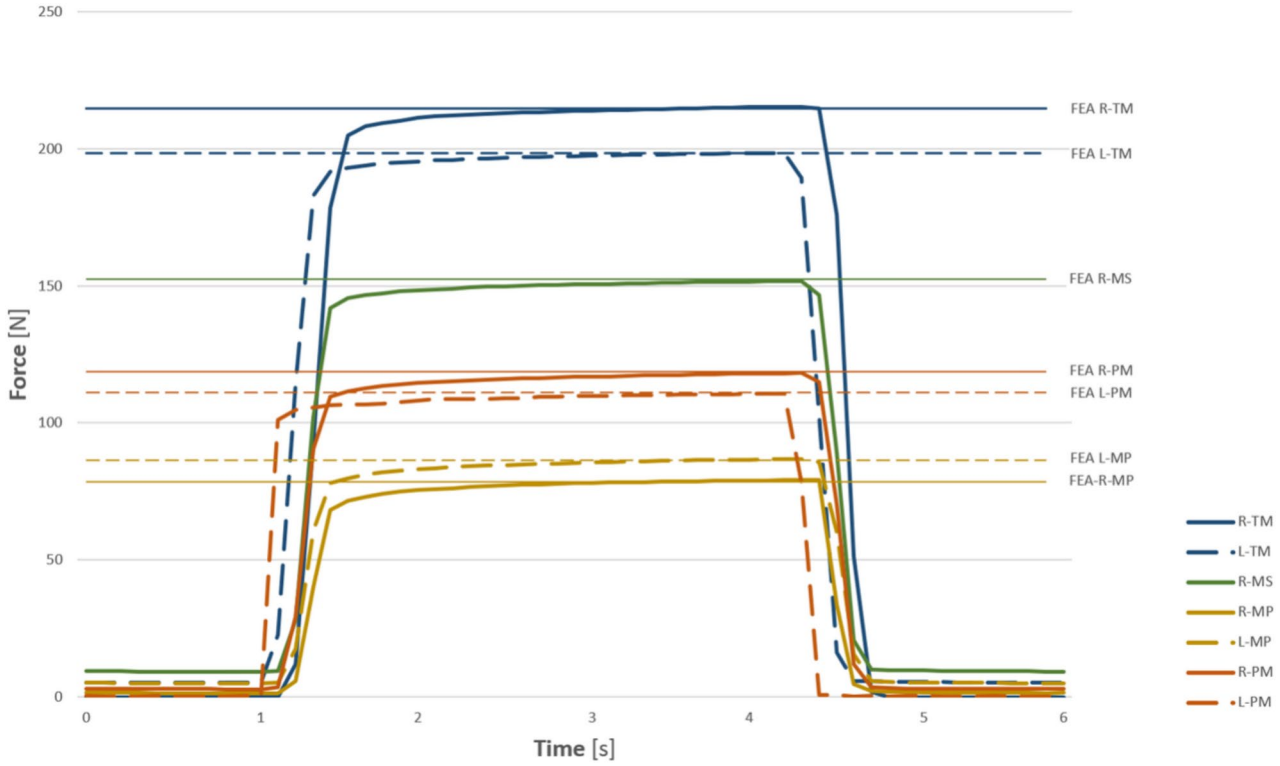

Fig. 6. Visualisation of the ramp-load used for the static validation of the MANDYBILATOR settings. The horizontal lines indicate the corresponding target values per muscle.

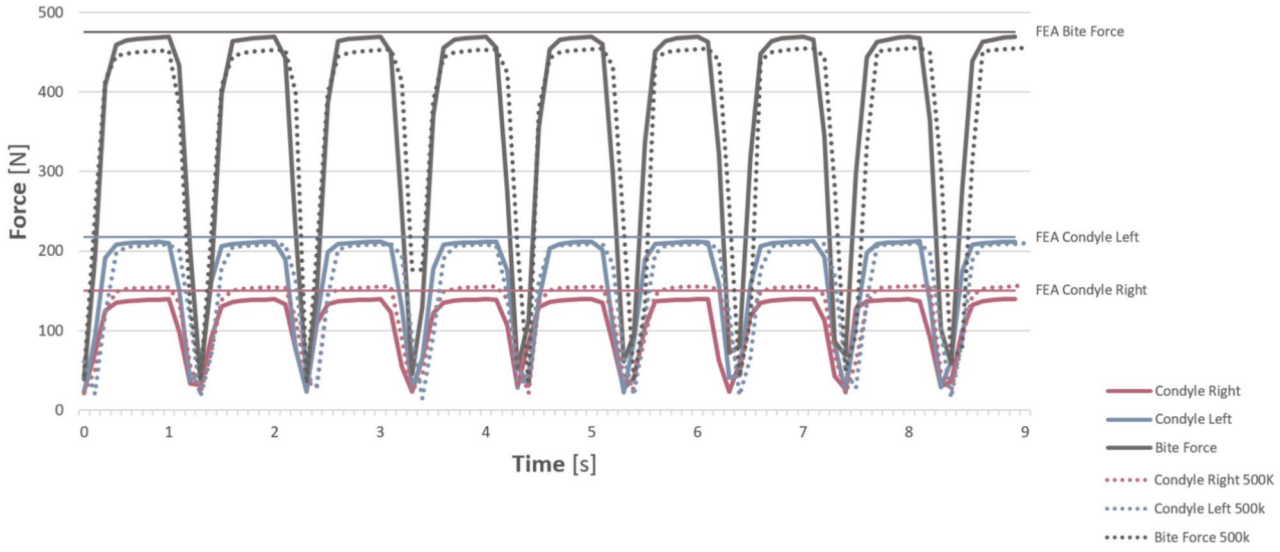

Fig. 7. Visualisation of the load cell outputs of both condylar forces and the molar bite force, generated by all the individually actuated elevator muscles of the MANDYBILATOR apparatus. The horizontal lines represent the corresponding forces that were derived from the FEA.

Static experiments

The three intact synthetic In-VitroBone mandible clones that functioned as baseline samples in the static test experiments, all showed similar failure modes as in all cases the condylar neck (2 × right, 1 × left) failed under the ultimate load. Failure occurred at 1309 N, 1114 N and 1380 N for samples 1, 2 and 3, respectively.

The topology optimisation procedure objectively removed only one of the 23 suggested screw positions. The remainder six ventral and 16 dorsal screws were used for the first two static PEEK reconstructed mandible tests samples. This resulted in ultimate failure at 1108 N for PEEK sample 1 and 1094 N PEEK sample 2. It was then

decided to only use four of the 16 dorsal screw positions in the third sample as this, clinically, would be a more reasonable number. PEEK sample 3 performed the best, failing at a load of 1212 N. In all three samples, the right condylar neck was the point of failure and the PEEK implants remained intact.

This resulted in a mean failure load of 1268 N (R:1114–1380 N) for the intact mandible samples and 1138 N (R:1094–1212) for the PEEK reconstructed samples.

The deformation of all six samples, three intact In-VitroBone mandibles and three PEEK reconstructed In-VitroBone mandibles, was measured at three corresponding points, i.e., the z-displacement of the force actuator, the external oblique line on the left side of the mandible and the pogonion. This resulted in a mean z-displacement of 3.36 mm (R:3.32–3.42) and 3.45 mm (R:3.27–3.81) for the intact and PEEK reconstructed In-VitroBone mandible samples respectively. The external oblique line measurements showed a mean displacement of 2.95 mm (R: 2.89–3.03) and 2.56 mm (R: 2.15–3.08) for the intact and PEEK reconstructed samples respectively and mean pogonion displacements of 2.98 mm (R: 2.25–3.62) and 2.96 mm (R: 2.39–3.42) for the intact and PEEK reconstructed samples respectively. Table 4 shows all the separate sample measurements. In Fig. 8, all the displacements are plotted against the compression force actuated in the z-direction.

Dynamic experiment

Regarding the fatigue experiment, it was decided to use only four out of the 16 screw options in the left ramus of the mandible as this appeared sufficient for the static experiment and also to stay close to the clinical situation. The PEEK reconstructed mandible survived the cyclic experiment and did not fail prior to the goal of 500,000 maximum molar bite force cycles, the equivalent of at least two years of in-vivo use. As the construct was still intact after the planned 500,000 cycle experiment had finished, it was decided to continue the experiment until failure occurred, or for1 million cycles. The experiment was stopped at 1.1 million cycles with no failure occurring or any visual signs of crack formation or screw loosening, as no rotation of the screw markings was observed.

Discussion

This study revealed that a topology optimised PEEK PSI for the reconstruction of large continuity defects can withstand the in-vivo loading of the mandible and can act as a substitute for titanium plates in the reconstruction of continuity defects of the mandible.

Our static experiments show that the ultimate strength of the In-VitroBone mandibles that were reconstructed with the PEEK implant are comparable to the unreconstructed intact In-VitroBone mandibles. All the PEEK implants remained intact and the failure mechanism of the PEEK reconstructed mandibles was the same as in the intact non-reconstructed samples. In all cases, the condylar neck fractured under ultimate load. The

	Sample	Intact	PEEK
Force [N]	n1	1309	1108
	n2	1114	1094
	n3	1380	1212
	mean	1268	1138
Z-displacement [mm]	n1	3.32	3.27
	n2	3.42	3.27
	n3	3.33	3.81
	mean	3.36	3.45
External oblique line [mm]	n1	2.93	2.45
	n2	2.89	2.15
	n3	3.03	3.08
	mean	2.95	2.56
Pogonion [mm]	n1	3.07	3.42
	n2	3.62	2.39
	n3	2.25	3.08
	mean	2.98	2.96

Table 4. The results of the static uniaxial compression testing of the PEEK reconstructed In-VitroBone mandibles versus the intact In-VitroBone samples on the MUNACAPP apparatus.
The ultimate compression force at failure was recorded together with the linear displacements at three points of the mandible: the z-displacement, which is the displacement of the load actuator, the external oblique line and the pogonion.

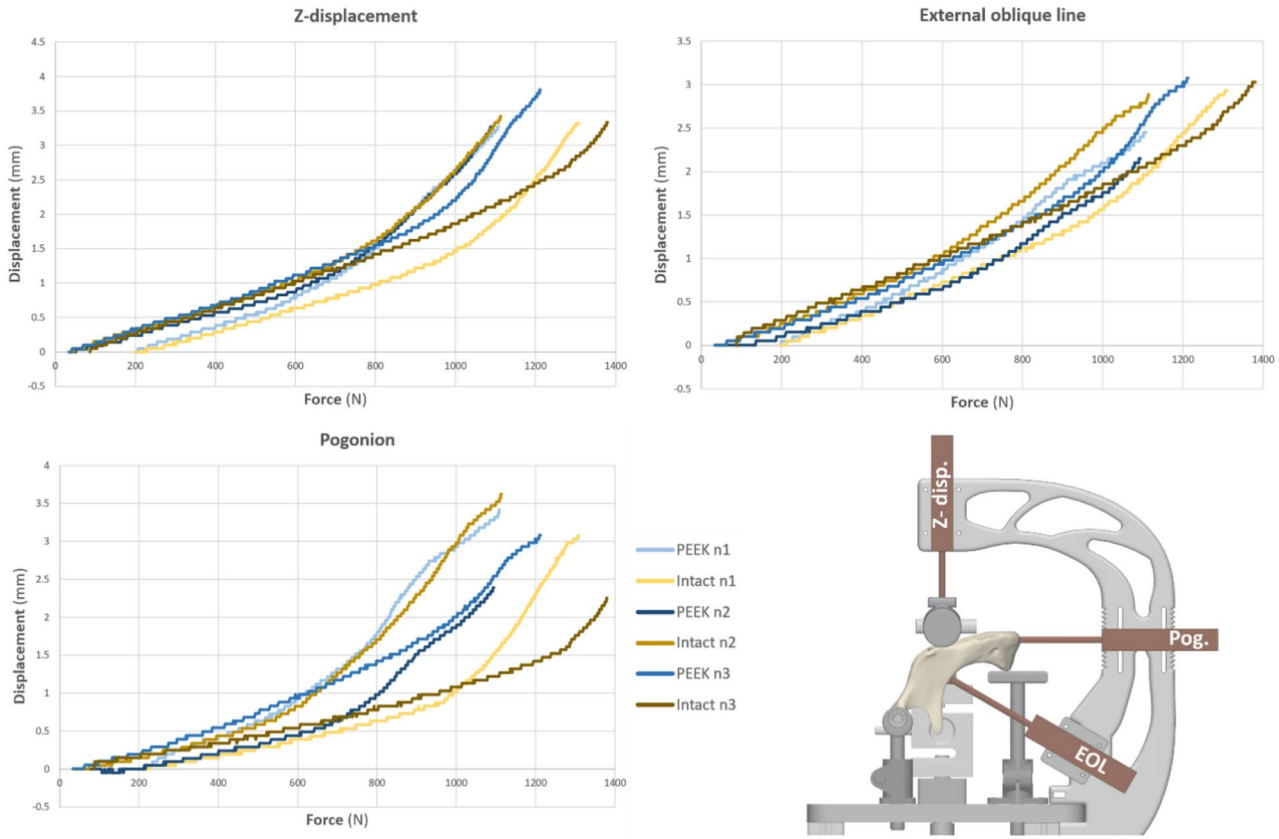

Fig. 8. Visualisation of the measured linear displacements at three positions on all the PEEK reconstructed mandible samples and all the intact mandible samples. The lower right image indicates the position and direction of the linear displacements.

dynamic, or cyclic, fatigue test we performed indicates that the PEEK implant is able to withstand multiple years (at least four/five years) of maximum in-vivo loading[13,34], which can be considered as clinically a long term, beyond the phase where most RPs fail[4].

To the best of our knowledge, only one other study has reconstructed a mandibular continuity defect using a PEEK implant[13]. In that study, however, the implant shape was directly copied from a titanium plate and therefore not specifically designed to function when manufactured from PEEK. As a result, they observed implant failure occurring at a mean force of 592 N as opposed to a mean of 1138 N observed with the PEEK implant reconstructed mandibles in our current study. Lommen et al.'s cyclic loading study[13] is in line with a number of studies presented in the literature[30–32]. They applied 300 N distributed over both mandibular angles for 250,000 cycles without implant failure. This load of 300 N, however, is not a realistic worst-case scenario representation of the in-vivo loading of the mandible. As we wanted to test our PEEK implants under the patient's physiological maximum load, we applied the PS muscle model obtained from MRI to the PEEK reconstructed mandible in our MANDYBILATOR apparatus. When mathematically converted into a single load at both mandibular angles to enable comparisons with, e.g., Lommen et al.'s study[13], the load of our dynamic experiment was equivalent to approximately 798 N applied to the angles. This resulted in a bite force of 443 N at the molar position, much higher than can generally be clinically expected from an edentulous patient[35].

As topology optimisation was applied to optimise the implant shape to the PS load conditions and PEEK's material properties, we could easily input and combine a number of load conditions. We used twelve different load scenarios to mimic the mouth opening and the bite positions throughout the dental arch. Topology optimisation is relatively new to the field of reconstructive implant design, especially in Oral and Maxillofacial surgery, but shows excellent potential for this application[14,32,36,37]. A great part of the otherwise subjective design process can be approached objectively and, using the correct PS inputs, e.g., muscle forces, directions and locations, leads to truly matching PS implants.

With the above in mind, we tried to objectify the otherwise subjective positioning of the implant screws. By adding a large number of screws (23), we expected the topology optimisation procedure would get rid of marginally loaded screw connections to the implant. This only worked in the front segment however, leaving 16 screws in the dorsal mandibular segment as the topology optimisation procedure had distributed the loads over all the potential screw positions. After manufacturing the PEEK implants and carrying out the first two static ultimate load tests, we only applied the four highest loaded screws to the third static test, according to our FEA analyses. This proved to be sufficiently strong, as this sample attained the highest ultimate load of all the PEEK

samples in the static experiments. Therefore, we decided to perform our dynamic testing in line with this last static experiment and only used four screws in the dorsal mandibular segment, as it would represent the clinical situation realistically. Two screws proved important to the total strength and success of the PEEK reconstruction. The 'Bookshelf' screw, as we presented in earlier research[19], together with the new 'dual-locking screw', which locks into the implant on both the buccal and lingual side of the mandible, play a role in the implant's resistance against medial flaring of the left mandibular segment, as an effect of partial removal of the masseter, and the overall torsion of the mandible under load. Connecting screws to mandibular implants on both buccal and lingual side has been performed in the past but this has been associated with bone resorption around the screw and ultimately loosening[20,21]. The main difference between these old applications of buccal bolts which were fixated lingually with nuts and our new 'dual-locking' principle, is that we added locking threads to both the buccal and lingual side of the implant, making it impossible for the screw to squeeze the mandible and initiate pressure related resorption.

The use of quasi-dynamic load scenarios to cover a range of bite positions and loading situations throughout the opening of the mandible in a FEA and subsequent topology optimisation appears to be an improvement over single static scenarios. In the current study, we applied different mouth opening positions and different bite locations in order to mimic the dynamic in-vivo bite options. By doing so, we found that the worst-case scenario, i.e., the scenario that influenced our PEEK implants design the most, was the molar bite due to amount of torsion this loading introduces into the implant in lateral continuity reconstructions. We therefore translated this load scenario to the dynamic cyclic test experiment.

As the subject of our exemplar case was already deceased, we could not determine the PS muscle model entirely conform our previously published protocol[22] due to lacking bite forces measurements. therefore, we chose to apply a slightly different muscle model to the FEA and subsequent topology optimisation, as was described in the Methods section. We used the PS MRI based muscle insertions and directions and combined these with the muscle forces from Langenbach and Hannam's study[23] to form a hybrid-muscle model, as these muscle forces are often reproduced in the literature as the input for FEAs of the mandible. Since we had tested intact In-VitroBone mandible samples to ultimate compression capacity, we were now interested in the equivalent compression force of this hybrid-muscle model, when translated to the MUNACAPP apparatus setup which we used for our static experiments. We found the equivalent compression force of 1364 N would represent our hybrid-muscle model. Comparing this value to the results of our static compression tests on the intact mandible models confirmed our expectations as two out of the three intact In-VitroBone mandible models had already failed, at 1268 N mean, prior to reaching the full force capacity of this hybrid-muscle model, with muscle forces taken from literature. This, together with the aforementioned ultimate strength of the In-VitroBone synthetic clones that matched the cadaveric mandibles within 1.5%, indicates that the muscle models that are often reproduced in the literature and taken as input for mandibular experiments are not universally applicable and might drastically overestimate the specific patient's muscle model. This might be an obvious statement but it plays a big role in the underestimation of, e.g., PEEKs potential as a material for reconstructive implants.

In 2004 Clason, Hinz and Schieferstein[38] published mechanical experiments on mandibles using their in-house developed device, called mandibulator. In order not to confuse the reader, it should be mentioned that this mandibulator device and our MANDYBILATOR apparatus are not the same and share no mutual development. The device of Clason, Hinz and Schieferstein was designed to load mandibles in static experiments. Forces were applied using sling around the dental arch and constraints were realised by means of a pterygo-massetric sling on either side. Their device formed the basis of three-point loading setups for static mechanical testing of the mandible. As aforementioned, such a device was found too over-simplified for our purpose and we developed our MANDYBILATOR apparatus for both PS static and dynamic experiments.

According to van Kootwijk et al.[32], it is very challenging to mimic the in-vivo three-dimensional loading configuration of the mandible and simplifications are, therefore, needed. This appears to be a popular conception in the literature, as performing uniaxial compression experiments on mandibles appears to be the golden standard[15,30–33]. In such simplified experiments, the mandible is generally placed on condylar supports while supporting a point of preference in the dental arch. A bar is used to apply a compression force to both mandibular angles to represent the effect of all jaw elevator muscles. By doing so, however, all the individual effects that the separate muscles have on the mandible, and possible implant, are ignored. For example, the mediolateral force equilibrium, that exists between the mediolateral force components of the masseter and medial pterygoid muscles, is disturbed upon removal of (a part) of either of the muscles. In the literature, the effect of muscle removal on the resection side of the mandible is generally approached by offsetting the load distribution on the left and right mandibular angles. As this only changes the force distribution in predominantly the cranial-caudal direction, it does not mimic the mediolateral imbalance on the mandibular ramus. Therefore, we decided to develop a novel and more complex testing apparatus that allows one to add all the patient-specific elevator muscles and provides information beyond the oversimplified and generally accepted gold standard setup. The dynamic experiment successfully reached its target cycle count of 500,000, and the MANDYBILATOR apparatus showed no signs of failure and exorbitant wear. As mentioned in the results section, the resultant forces at both condyles and at the molar bite location did not deviate more than 10% from the initially setup values, which we consider consistent considering the number of influencing components and sensors. The 500,000 cycles target of the dynamic experiment was based on the highest number of cycles we found in the literature for mandibular testing[16]. The bulk of the cyclic experiments, generally using the aforementioned oversimplified uniaxial setup, ran up to a maximum of 250,000 cycles[15,30–33] but the rationale behind this number of cycles was not presented. We expect this number was taken from a study in which the duration of the experiment was based on stress–strain curves for titanium or another metal in combination with a specific loading force. As we were not testing a metallic implant in the current study, we decided to use 500,000 as the target cycle count and even let the experiment continue to well past 1 million cycles (1.1 million). As already mentioned, this represents at least

four to five years of maximum in-vivo loading[13,34], where every moderate bite was assumed to represent the patient's maximum bite capacity. This is not the more likely scenario as the greatest amount of time is usually spent on chewing at lower pressures and higher pressures are only used for brief periods[39].

Within these four to five years, according to Maurer et al.[4], it is likely that if screw loosening were to occur in a reconstruction, it would have occurred already, within the first six months postoperatively. Also reconstruction plate failure due to metallic implants fracture generally occurs already within the first one to five years postoperatively[2,5].

As PEEK has a number of derivatives within the PAEK family as well as composites[40–42], future work should aim to reevaluate our choice for applying PEEK in this study and focus on gathering insights on the biological response of the hard and soft tissues to the implanted PAEK (composite) implant of choice. Cell adhesive potentials and antibacterial properties should be explored as we think these are important in the prevention of and coping with dehiscence of the reconstructions of continuity defects of the mandible. Furthermore, the effect of the implant-surrounding tissues on the irradiated implant after radiotherapy remains unknown and should be explored as well.

Conclusions

As hypothesised, a full PEEK PS implant obtained through thorough finite element analysis and subsequent topology optimisation, and provided with strategically placed screws, can withstand comparable forces to that of in-vivo loading of the mandible. It has the mechanical potential to act as a substitute for the current titanium plates used in the reconstruction of continuity defects of the mandible. This may potentially lead to optimised patient-specific reconstructions, with the implants matching the bone's stiffness and possessing radiolucent properties which are useful for radiographic follow-ups and radiotherapy. Furthermore, the addition of the dynamic/cyclic MANDYBILATOR apparatus to the common (static) uniaxial mechanical testing setup allows for more realistic application of the in-vivo loading of the mandible and can provide added insights in biomechanical behaviour of the mandible.

Data availability

The data that support the findings of this study are available from the corresponding author upon reasonable request.

Received: 24 June 2024; Accepted: 10 December 2024
Published online: 03 January 2025

References

1. Gellrich, N. C. et al. Comparative study of locking plates in mandibular reconstruction after ablative tumor surgery: THORP versus UniLOCK system. *J. Oral Maxillofac. Surg.* **62**, 186–193 (2004).
2. Katakura, A., Shibahara, T., Noma, H. & Yoshinari, M. Material analysis of AO plate fracture cases. *J. Oral Maxillofac. Surg.* **62**, 348–352 (2004).
3. Lopez, R., Dekeister, C., Sleiman, Z. & Paoli, J. R. Mandibular reconstruction using the titanium functionally dynamic bridging plate system: A retrospective study of 34 cases. *J. Oral Maxillofac. Surg.* **62**, 421–426 (2004).
4. Maurer, P., Eckert, A. W., Kriwalsky, M. S. & Schubert, J. Scope and limitations of methods of mandibular reconstruction: A long-term follow-up. *Br. J. Oral Maxillofac. Surg.* **48**, 100–104 (2010).
5. Shibahara, T., Noma, H., Furuya, Y. & Takaki, R. Fracture of mandibular reconstruction plates used after tumor resection. *J. Oral Maxillofac. Surg.* **60**, 182–185 (2002).
6. Vitins, V., Dobelis, M., Middleton, J., Limbert, G. & Knets, I. Flexural and creep properties of human jaw compact bone for FEA studies. *Comput. Methods Biomech. Biomed. Eng.* **6**, 299–303 (2003).
7. Xin, P. et al. Material assignment in finite element modeling: Heterogeneous properties of the mandibular bone. *J. Craniofacial Surg.* **24**, 405–410 (2013).
8. Frost, H. M. Bone, "mass" and the "mechanostat": a proposal. *Anat. Rec.* **219**, 1–9 (1987).
9. Frost, H. M. Bone's mechanostat: a 2003 update. *Anat. Rec. A. Discov. Mol. Cell. Evol. Biol.* **275**, 1081–1101 (2003).
10. Gefen, A. Computational simulations of stress shielding and bone resorption around existing and computer-designed orthopaedic screws. *Med. Biol. Eng. Comput.* **40**, 311–322 (2002).
11. Lommen, J. et al. Reduction of CT artifacts using polyetheretherketone (PEEK), polyetherketoneketone (PEKK), polyphenylsulfone (PPSU), and polyethylene (PE) reconstruction plates in oral oncology. *J. Oral Maxillofac. Surg.* **80**, 1272–1283 (2022).
12. Rendenbach, C. et al. Patient specific glass fiber reinforced composite versus titanium plate: A comparative biomechanical analysis under cyclic dynamic loading. *J. Mech. Behav. Biomed. Mater.* **91**, 212–219 (2019).
13. Lommen, J. et al. Mechanical fatigue performance of patient-specific polymer plates in oncologic mandible reconstruction. *J. Clin. Med.* **11**, 3308. https://doi.org/10.3390/jcm11123308 (2022).
14. Sutradhar, A. et al. Designing patient-specific 3D printed craniofacial implants using a novel topology optimization method. *Med. Biol. Eng. Comput.* **54**, 1123–1135 (2016).
15. Koper, D. C. et al. Topology optimization of a mandibular reconstruction plate and biomechanical validation. *J. Mech. Behav. Biomed. Mater.* **113**, 104157 (2021).
16. Lang, J. J. et al. Improving mandibular reconstruction by using topology optimization, patient specific design and additive manufacturing?-A biomechanical comparison against miniplates on human specimen. *PLoS One* **16**, e0253002 (2021).
17. Brown, J. S., Barry, C., Ho, M. & Shaw, R. A new classification for mandibular defects after oncological resection. *Lancet Oncol.* **17**, 23 (2016).
18. Jewer, D. D. et al. Orofacial and mandibular reconstruction with the iliac crest free flap: A review of 60 cases and a new method of classification. *Plast. Reconstr. Surg.* **84**, 391–395 (1989).
19. Merema, B. B. J. *et al.* Novel finite element-based plate design for bridging mandibular defects: Reducing mechanical failure. *Oral Dis.* (2020).
20. Winter, L. & McQuillan, A. S. Embedment of a Vitallium mandibular prosthesis as an integral part of the operation for removal of an adamantinoma. *The American Journ. of Surgery* **LXIX**, 318–324 (1945).
21. Freeman, B. S. The use of Vitallium plates to maintain function following resection of the mandible. *Plast. Reconstr. Surg.* **1946**(3), 73–78 (1948).

22. Merema, B. B. J., Sieswerda, J. J., Spijkervet, F. K. L., Kraeima, J. & Witjes, M. J. H. A contemporary approach to non-invasive 3D determination of individual masticatory muscle forces: a proof of concept. *J. Pers. Med.* **12**, 1273. https://doi.org/10.3390/jpm12081273 (2022).
23. Langenbach, G. E. & Hannam, A. G. The role of passive muscle tensions in a three-dimensional dynamic model of the human jaw. *Arch. Oral Biol.* **44**, 557–573 (1999).
24. Weijs, W. A. & Hillen, B. Cross-sectional areas and estimated intrinsic strength of the human jaw muscles (1986).
25. Mesnard, M. & Ramos, A. Experimental and numerical predictions of Biomet((R)) alloplastic implant in a cadaveric mandibular ramus. *J. Craniomaxillofac. Surg.* **44**, 608–615 (2016).
26. Mesnard, M. et al. Biomechanical analysis comparing natural and alloplastic temporomandibular joint replacement using a finite element model. *J. Oral Maxillofac. Surg.* **69**, 1008–1017 (2011).
27. Ramos, A., Ballu, A., Mesnard, M., Talaia, P. & Simões, J. Numerical and experimental models of the mandible. *Exp. Mech.* **51**, 1053–1059 (2011).
28. Ramos, A. M. & Mesnard, M. The stock alloplastic temporomandibular joint implant can influence the behavior of the opposite native joint: A numerical study. *J. Cranio-Maxillofacial Surg.* **43**, 1384–1391 (2015).
29. Ramos, A., Nyashin, Y. & Mesnard, M. Influences of geometrical and mechanical properties of bone tissues in mandible behaviour - experimental and numerical predictions. *Comput. Methods Biomech. Biomed. Eng.* **20**, 1004 (2017).
30. Schupp, W., Arzdorf, M., Linke, B. & Gutwald, R. Biomechanical testing of different osteosynthesis systems for segmental resection of the mandible. *J. Oral Maxillofac. Surg.* **65**, 924–930 (2007).
31. Gutwald, R., Jaeger, R. & Lambers, F. M. Customized mandibular reconstruction plates improve mechanical performance in a mandibular reconstruction model. *Comput. Methods Biomech. Biomed. Eng.* **20**, 426–435 (2017).
32. van Kootwijk, A. et al. Semi-automated digital workflow to design and evaluate patient-specific mandibular reconstruction implants. *J. Mech. Behav. Biomed. Mater.* **132**, 105291 (2022).
33. Gateno, J. et al. Biomechanical evaluation of a new MatrixMandible plating system on cadaver mandibles. *J. Oral Maxillofac. Surg.* **71**, 1900–1914 (2013).
34. Wu, C. H., Lin, Y. S., Liu, Y. S. & Lin, C. L. Biomechanical evaluation of a novel hybrid reconstruction plate for mandible segmental defects: A finite element analysis and fatigue testing. *J. Craniomaxillofac. Surg.* **45**, 1671–1680 (2017).
35. Tripathi, G. et al. Comparative evaluation of maximum bite force in dentulous and edentulous individuals with different facial forms. *J. Clin. Diagn. Res.* **8**, ZC37-40 (2014).
36. Lemón, L. Topology optimization process for new designs of reconstruction plates used for bridging large mandibular defects (2016).
37. Li, C. H., Wu, C. H. & Lin, C. L. Design of a patient-specific mandible reconstruction implant with dental prosthesis for metal 3D printing using integrated weighted topology optimization and finite element analysis. *J. Mech. Behav. Biomed. Mater.* **105**, 103700 (2020).
38. Clason, C., Hinz, A. M. & Schieferstein, H. A method for material parameter determination for the human mandible based on simulation and experiment. *Comput. Methods Biomech. Biomed. Eng.* **7**, 265–276 (2004).
39. Bates, J. F. & Stafford, G. D. Masticatory function-a review of the literature: (II) Speed of movement of the mandible, rate of chewing and forces developed in chewing. *J. Oral Rehabil.* **2**, 349–361 (1975).
40. Almasi, D. et al. Preparation methods for improving PEEK's bioactivity for orthopedic and dental application: A review. *Int. J. Biomater.* **2016**, 8202653 (2016).
41. Zhao, M. et al. Response of human osteoblast to n-HA/PEEK–quantitative proteomic study of bio-effects of nano-hydroxyapatite composite. *Sci. Rep.* **6**, 22832 (2016).
42. Ma, R. & Guo, D. Evaluating the bioactivity of a hydroxyapatite-incorporated polyetheretherketone biocomposite. *J. Orthop. Surg. Res.* **14**, 32–41 (2019).

Acknowledgements

The authors are thankful for the help provided by our colleagues of the Anatomy Laboratory facility in the University Medical Center Gronigen, The Netherlands.

Author contributions

B.M.: Conceived and designed the work that led to the submission, acquired data, and played an important role in interpreting the results, drafted the manuscript and approved the final version. F.S.: Played an important role in interpreting the results, revised the manuscript and approved the final version. J.K.: Designed the work that led to the submission, played an important role in interpreting the results, revised the manuscript and approved the final version. MW: Designed the work that led to the submission, played an important role in interpreting the results, revised the manuscript and approved the final version. All author gave their final approval and agree to be accountable for all aspects of the work.

Declarations

Competing interests

The authors declare no competing interests.

Ethical approval

The subject provided their written informed consent and patient anonymity has been maintained using only the anonymised CT-imaging. Usage has been approved by the medical ethics committee of the University Medical Center Groningen (UMCG METC approval 2010/109). Cadaveric material was provided by the Anatomy department of the University Medical Center Groningen, after approval of the experimental protocol, and used in their lab under strict supervision.

Data usage

All methods were carried out in accordance with relevant guidelines and regulations.

Additional information

Correspondence and requests for materials should be addressed to B.B.J.M.